SNOW DEPTH MAPPING IN THE ALPS: MERGING OF *IN SITU* AND REMOTELY-SENSED DATA

Nando Foppa[1], Andreas Stoffel [2] and Roland Meister [2]

1. University of Bern, Department of Geography, Bern, Switzerland; foppa(at)giub.unibe.ch
2. Swiss Federal Institute for Snow and Avalanche Research, Davos, Switzerland; {stoffel/meister}(at)slf.ch

ABSTRACT

The Swiss Federal Institute for Snow and Avalanche Research in Davos (SLF) publishes daily snow and avalanche information including snow depth maps on a spatial resolution of 1×1 km^2 for Switzerland. These maps are generated using a spatial interpolation technique based on snow station measurements. Although the station network has become denser over the past years, several regions do not contribute well to the network. The U.S. National Oceanic and Atmospheric Administration (NOAA) Advanced Very High Resolution Radiometer (AVHRR) sensor is used to improve the information on snow-covered ground. The fusion of point measurements with small-scale remote sensing data leads to an improved area-wide snow information. The presented merging technique based on virtual snow stations is applied for a case study on the Swiss Alps on 4 January 2005. The combination technique is a new approach and the resulting nation-wide snow depth maps show a significant improvement compared to the conventional interpolation with a more accurate snow – no snow borderline. The interpolation method seems to be sensitive to an accurate snow – no snow classification of the satellite data. The preliminary results are very promising and a near-real time application is already in operational use. Ongoing work is concentrating on the validation of the snow cover maps and improvements to the spatial interpolation method.

Keywords: NOAA-AVHRR, snow cover, snow depth.

INTRODUCTION

Monitoring snow depth in the Swiss Alps has a long tradition. These measurements provide a basis for avalanche forecasting, hydrological snowmelt runoff modelling and they are an important source of information for winter tourism. The Swiss Federal Institute for Snow and Avalanche Research in Davos (SLF) publishes daily information about the avalanche situation and the snow conditions in the Swiss Alps. In addition to avalanche, text bulletins, country-wide maps for avalanche danger, snow pack stability, new snow depth and snow depth are primary products of the institute's snow information.

Snow depth is measured at more than 250 snow and weather stations in Switzerland, mainly in the alpine region. These point measurements are used to interpolate area-wide snow depth maps for Switzerland. Different authors published interpolation approaches to accomplish this task. Witmer (1) developed a method to calculate an area-wide snow depth value taking into account regional and topographical influences. These snow depth maps were based on a linear dependency of snow depth and altitude for seven predefined climatological regions. This approach has been adapted for altitudes lower than 2500 m a.s.l. and published in the Climatological Atlas of Switzerland (2). There, snow depth mapping is based on 160 snow stations over the time period from 1961 to 1980. Kirchhofer (3) also used a simple linear technique but with monthly mean snow depth from December to March over the longer period of 1961 to 1990.

Since 1989 a similar approach has been used at the SLF where the snow depth is calculated for a given base elevation (e.g. 1500 m a.s.l.). Auer (4) developed a new model, which does not rely on predefined regions. An area-wide base value is determined and adjusted by a regional-to-local compensation value. The resulting snow depth map is calculated on a grid cell size of 1×1 km^2

over Switzerland. First results of this modelling method show more accurate and realistic snow depth values than in the old maps, with a well-defined snow – no snow borderline. Especially in regions with a dense network of snow stations the interpolation method is fairly accurate. However the number of operational snow stations varies during the winter season. This is the case in early winter and in spring when the snow observations in lower altitudes are not operated. Therefore, an additional snow information source is included by the use of real-time snow cover maps from satellite data. The combination of interpolated snow depth values and the snow cover extent provided from satellite data is a challenging task, as the two data sets consist of different spatial scales with a different view on the object snow.

In this paper, we describe and analyse the retrieval of snow depth maps in combination with operational snow cover maps generated from satellite images. The study includes the entire area of Switzerland representing different topography and land cover types.

DATA

In situ snow depth data

In Switzerland snow depth is measured by the SLF and the national weather service MeteoSwiss. The SLF operates two different types of networks, the conventional observation stations and the automatic snow and weather stations. The SLF conventional observation stations are generally located at alpine villages and ski resorts. Their observation program goes beyond purely meteorological parameters. Beside weather information, new snow and snow depth measurements, a variety of other snow parameters are observed and recorded on a daily basis. The SLF automatic snow and wind stations are situated at altitudes above about 2000 m a.s.l., close to avalanche starting zones. MeteoSwiss also operates a man-operated network and an automatic measurement network. The MeteoSwiss observer stations are mainly situated at lower elevations below about 1000 m a.s.l. more or less evenly distributed over the country. The MeteoSwiss automatic snow stations were built in co-operation with the SLF. These snow stations are located at higher altitudes above about 2000 m a.s.l. regularly distributed over the Swiss Alps. Figure 1 shows the location of all snow stations in winter 2004/2005. The total number of snow stations is 253, whereof 5 to 10% may be out of order on a certain day. The total number of snow measurements is greatly reduced in early winter and spring due to a shorter period of observation of the observation stations at lower altitudes.

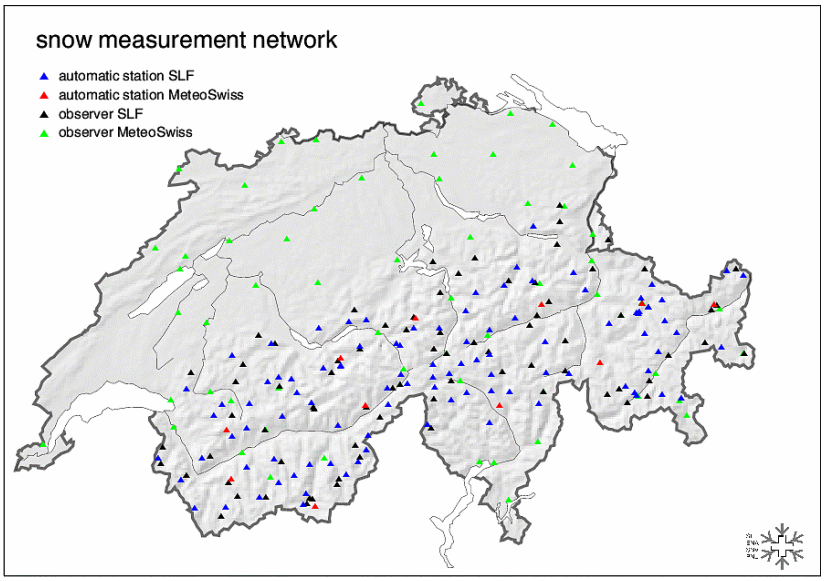

Figure 1: Swiss snow measurement network.

Satellite data

The operational polar orbiting NOAA satellites provide daily images from the AVHRR (Advanced Very High Resolution Radiometer) scanner with 1.1 km spatial resolution. The AVHRR scanner has five spectral bands measuring reflected solar (visible and near-infrared) energy and emitted thermal energy from the earth's surface and the atmosphere. The Remote Sensing Research Group at the University of Bern, Switzerland, receives and archives NOAA-AVHRR HRPT data covering the area of the whole European Alps from 40.5°N to 50°N and 0°E to 17°E. Since the beginning of 2002, an operational status to process the data in near real-time has been in use.

In the presented paper, NOAA-17 morning passes are used due to the illumination conditions in winter and the advantage of the purely reflective channel 3A (1.6 μm) for an improved snow/cloud discrimination. Additionally, we are dealing with channel 1 (0.6 μm) and 2 (0.9 μm). The pre-processing includes calibration according to the KLM User's Guide (5), georeferencing including a feature-matching algorithm to geocode the satellite data with sub-pixel accuracy and an atmospheric correction of the visible channels 1 and 2. Atmospheric correction is based on the SMAC algorithm (Simplified Method for Atmospheric Corrections) (6). Atmospheric parameters are derived from the NCEP data sets (National Center for Environmental Prediction) and from the Alpine Model (aLMo) of MeteoSwiss, whereas the atmospherical aerosol content is extracted from the same AVHRR data set processed. Data sets are orthorectified using the terrain model GTOPO30. This is an essential step to take into consideration the geometric distortions introduced by the complex topography and the scan geometry. Cloud detection and masking are done using the Cloud and Surface Parameter Retrieval (CASPR) package (7).

METHODS

Snow depth interpolation

The spatial distribution of the snow depth varies for different scales, but is dominated by altitude and is secondarily influenced by topographical parameters such as slope and aspect due to differences in incoming solar radiation and wind. These terrain characteristics have an effect on snow depth especially at lower altitudes mainly due to the difference in incoming solar radiation between north-facing and south-facing slopes (1). The factors depend on the weather situation and the radiation intensity varies on a high temporal and spatial resolution, which makes a determination on a 1 km grid size difficult. A nation-wide study of the alpine surface radiation budget is ongoing work and might contribute to understand the impact of slope and aspect on the snow depth in different elevation zones.

In this study we present a spatial interpolation method, which is based on the dependency of snow depth and altitude above sea level as well as the local and regional characteristics of the snow distribution.

The algorithm incorporates two steps.

First, the country-wide base value is determined, which describes the correlation between the snow depth and altitude for two elevation zones above and below 1300 m. This linear function represents the dependency of snow depth and altitude as an overall function for whole Switzerland. This general description is an approximation explaining 50-70% of the total variance of the snow depth with the variable altitude.

Therefore, the base value is adjusted with a local to regional compensation factor in a second step. This results in the following general formula:

$$HS_j = G(h_j) + A_j \quad (1)$$

where:
- *HS:* snow depth in cm
- *G:* base value in cm
- *A:* compensation value in cm

h: altitude of the grid cell in m a.s.l.
j: grid cell to be calculated

The compensation value is added to the base value to adjust the snow depth value for each cell in the 1×1 km^2 grid. This compensation value is calculated by inverse distance weighting of the difference of the base value and the measured value for the three stations nearest to the grid cell. Consequently the formula for the compensation value is:

$$A_j = \frac{h_j}{\sum_{i=1}^{3}\left(\frac{1}{d_{ji}}\right)} \cdot \sum_{i=1}^{3}\left[\frac{1}{d_{ji}}\frac{(HS_i - G(h_i))}{h_i}\right] \qquad (2)$$

where:
h_j: altitude of the grid cell *i* in m a.s.l.
d_{ji}: distance between grid cell *j* and observation station *i* in km
HS_i: measured snow depth at observation station *i* in cm
$G(h_i)$: base value of modelled snow depth at the observation station in cm
h_i: altitude of the observation station in m a.s.l.
j: grid cell *j*, to be varied at a 1 km grid over the whole area
i: observation station *i*, *i*=3 and minimum distance to the grid cell *j*.

An example for the application of this spatial interpolation method with *in situ* snow depth data from January 4, 2005 is shown in Figure 5.

Snow cover maps from satellite data

The medium spatial resolution of the AVHRR sensor of 1.1 km at nadir is a challenge in rugged relief with small patches of snow and a heterogeneous land surface. Due to this effect, each pixel potentially represents a mixture of different land cover types. To overcome this difficulty, snow cover proportions within a pixel are calculated. The estimation of snow information at sub-pixel scale is presented in different papers (8,9,10,11). Satellite imagery from different sensors have been used for estimating fractional snow cover within a sensor pixel (12,13). The linear spectral mixture algorithm is one of the most commonly used techniques to estimate snow cover proportions and has proven to be effective at local to regional scales as well as in alpine topography (14).

Linear mixture modelling (15) is based on the assumption that the signal received at the sensor is a linear mixture of pure-element reflections called endmembers. The weights of these endmembers represent the percentage of the pixel area occupied by each ground cover type. The weighting coefficients (fractions) are constrained to be physically meaningful e.g. non-negative and sum to one. The system is solved by a least-square solution to minimize the unmodelled sum of squares of errors. The endmember selection is a crucial step in the spectral mixture analysis approach.

In the presented processing, the endmember selection and spectra mixture modelling is scene based. First, a Principal Component Analysis (PCA) is used to remove spectral redundancy and to improve the spectral separability. The first two eigenchannels of the first three AVHRR/3 channels contain considerably more than 90% of the total variance. This method requires no *a priori* knowledge of the data set or spectral properties of the land cover types. The concept of convex geometry introduced first by Settle and Drake (16) is based on the assumption that points lying on the outer line of a polygon surrounding the data cloud have the purest image spectra, whereas mixed pixels lie within the data space. Some of these points represent snow by their spectral signature and differ substantially from other pure spectra. The maximum number of endmembers is limited by the number of spectral bands of the sensor used. In this case, either endmember pairs or triples could be built. The use of endmember pairs is computationally less demanding but implicates to partition unmodelled endmembers into fractions, creating a fraction error. Sets of image endmember pairs are built consisting of the selected snow endmember and an additional unknown image endmember which is not further analysed. The number of endmembers and the snow image endmember are fixed, whereas one endmember type can vary. These endmember combinations are

used to describe all the pixels in the AVHRR data set. By creating multiple endmember combinations, the spectral variability of an image element is more effectively taken into account (17). The data set is unmixed using all endmember combinations. The output of each mixing model is a fraction image of the unknown endmember and the snow endmember. In addition, a root mean squared (RMS) error image represents the modelling error for each pixel. The fraction of snow in a specific pixel corresponds to the model with the lowest RMS for this image element. The described procedure is an automatically straightforward approach for operational and near real-time applications. Further information on the separated processing steps and a discussion of the method is described by (18).

Merging of *in situ* snow depth data with satellite data

The process of combining measured snow depth data with the snow cover extent from satellite data to calculate an area-wide snow depth map is a complex process and presented here for the first time. The aim is to improve the area-wide snow depth interpolation by the use of operational snow cover maps to refine the snow depth maps at the snow – no snow borderline. One must keep in mind that the two data sets consist of different spatial scales. A direct intersect of the two data sets was analysed but rejected, because a smooth transition of the snow depth is not achievable and because the cloud coverage in the satellite data leads to further implementation problems. The satellite snow cover data gives important information as to the extent of the snow-free area where the snow measurements are sparse. The definition of snow-free pixels from the AVHRR sub-pixel snow cover map is a crucial factor, as almost each pixel contains a certain amount of snow. The modelling constraints and the two-endmember model are responsible for this effect, as each pixel is unmixed using a snow spectra which might not even exist in the corresponding pixel. Figure 2 shows the histogram of the snow cover proportions from all cloud-free pixels in the presented data set.

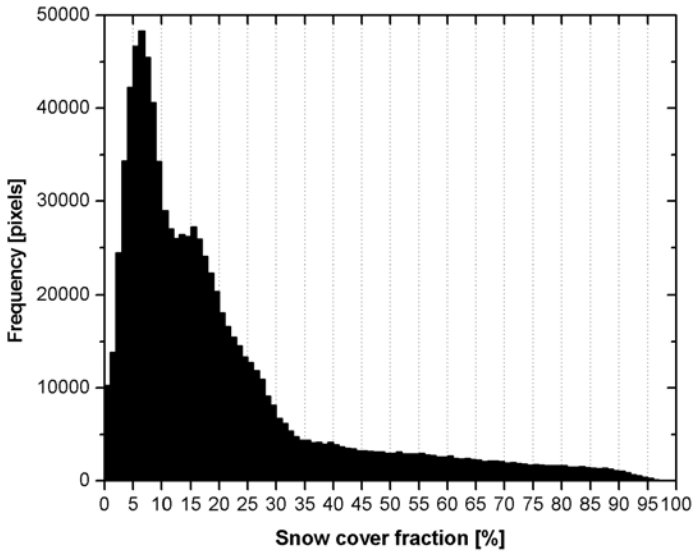

Figure 2: Frequency distribution of the sub-pixel snow values from the snow cover map processed on January 4, 2005, 09:53 UTC.

It is obvious that the histogram has a non-uniform distribution with a peak at the lower end of the snow cover fraction scale. The frequency distribution of pixels from several regions assumed to be totally snow-free has a normal distribution pattern of snow fraction values. Therefore, we define a threshold of two times the snow cover value of this peak. All pixels with a snow cover proportion below this value are labelled snow-free. In this case the threshold is set at a snow cover fraction value of 15%.

First attempts of merging the two data sets were made with a regular grid at a cell size of 5 and 10 km. All grid points were intersected with the binary snow cover map and the points with no snow values were entered as virtual snow stations with a zero snow depth value into the snow depth

interpolation. All other virtual snow stations were not included in the calculation. The test results for the 5 km grid were very promising, but the computation time exceeded the requirements of an interactive application. The 10 km grid was too coarse to improve the snow depth interpolation model. The regular grid approach was also too restraining, because many points were located at places at higher elevations, where the snow cover is more likely to last. Thus, a new approach was followed to gain an irregular network of points along the course of the main rivers (see Figure 3).

At these lower elevations the snow cover season is in general short which will result in a larger number of virtual snow stations to feed the snow depth interpolation model. This approach leads to an improved snow depth calculation with an acceptable computation time.

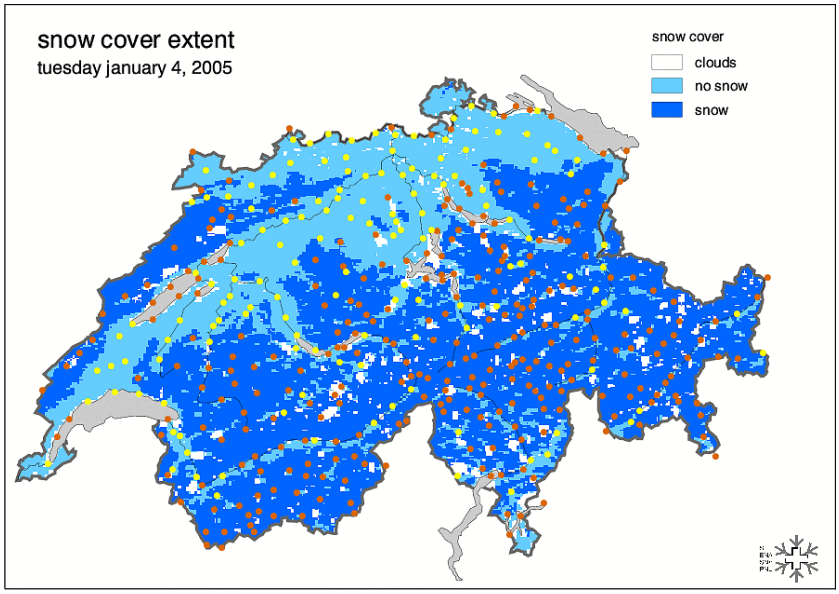

Figure 3: Binary snow cover map using a threshold of 15% snow cover fraction. The virtual snow stations are displayed, whereof the yellow points are classified to no snow with a snow depth of 0 cm in the interpolation method. A binary water mask and cloud mask is used to exclude corresponding pixels from the interpolation process.

RESULTS

The described approach is presented for a data set of January 4, 2005 in the following. Switzerland is almost cloud-free on that day, as seen in the NOAA AVHRR image in Figure 4.

The resulting binary snow cover map generated from the sub-pixel snow information shows a nearly closed snow cover in the alpine region and the prealps of Switzerland. The area-wide snow depth map was calculated with and without the use of the satellite data. The following figures show a series of maps that clearly express the influence of merging the measured snow depth with the snow cover extent from satellite data. In Figure 5, calculated with snow depth measurements only, the snow cover is extending further into the low lands. High snow depth values are found in the central Swiss Alps, especially in the eastern part of the northern slope of the Alps and in the southern part of the Alps next to the Lake Maggiore. In general the snow depth situation is below average for this time of the year.

In Figure 6, calculated by using the satellite data, the snow–no snow border fits closer to the snow cover extent gained from the satellite data and the overestimated snow depth values in the regions mentioned above disappeared.

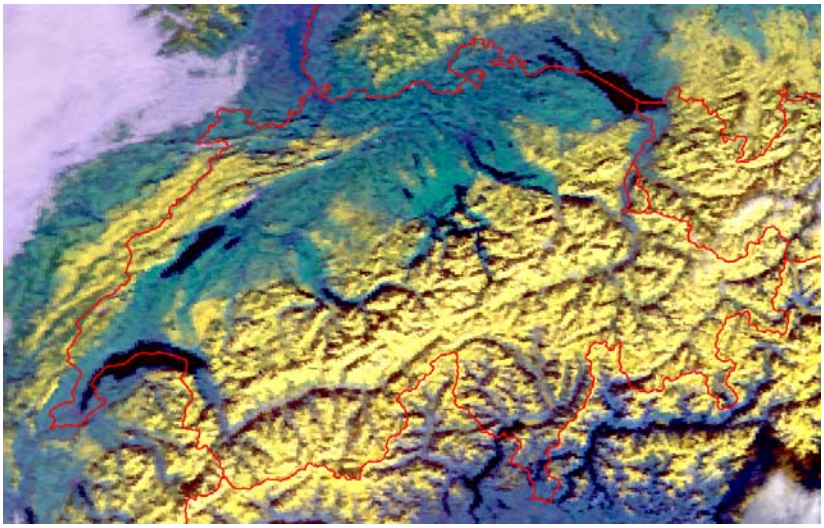

Figure 4: The Swiss Alps viewed from the NOAA-17 by the AVHRR sensor on January 4, 2005, 09:53 UTC (False colour composite, R: Channel 1, G: Channel 2, B: Channel 3).

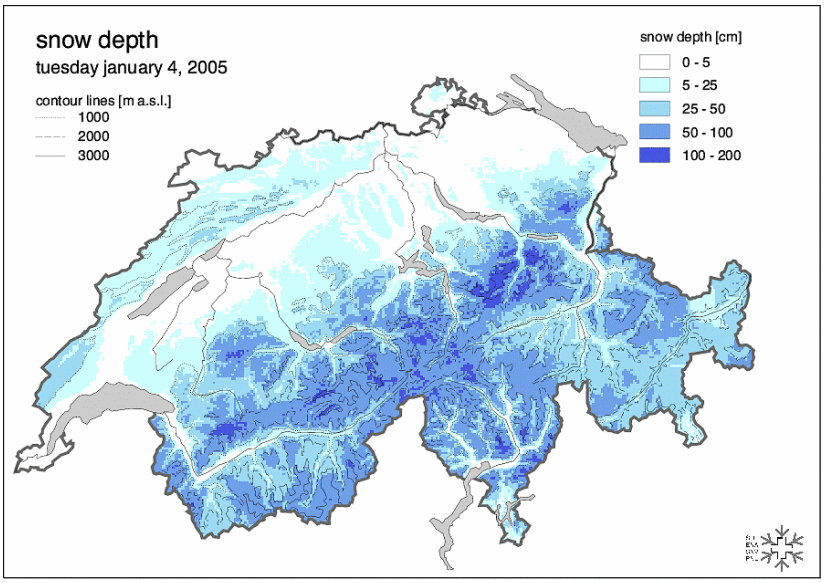

Figure 5: Snow depth map calculated with in situ *snow depth data only.*

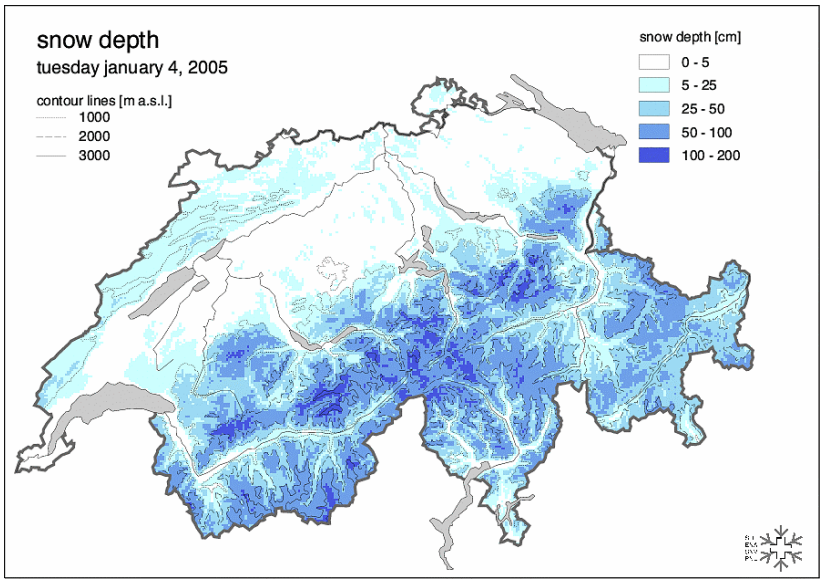

Figure 6: Snow depth map calculated with in situ *snow depth data and no snow values from satellite data.*

The difference calculated from data in Figure 5 minus those in Figure 6 is shown in Figure 7 and allows a more detailed analysis of the two calculations. The red colours indicate areas where the snow depth increased with the introduction of the virtual snow stations extracted from the satellite snow cover extent. These areas are mainly found at higher elevations but also in the north-eastern part of Switzerland. The blue areas, however, indicate regions with decreased snow depth. These are mainly located in lower elevation zones of the central lowland as well as at high altitudes of southern and eastern Switzerland. These areas are subject to further analysis.

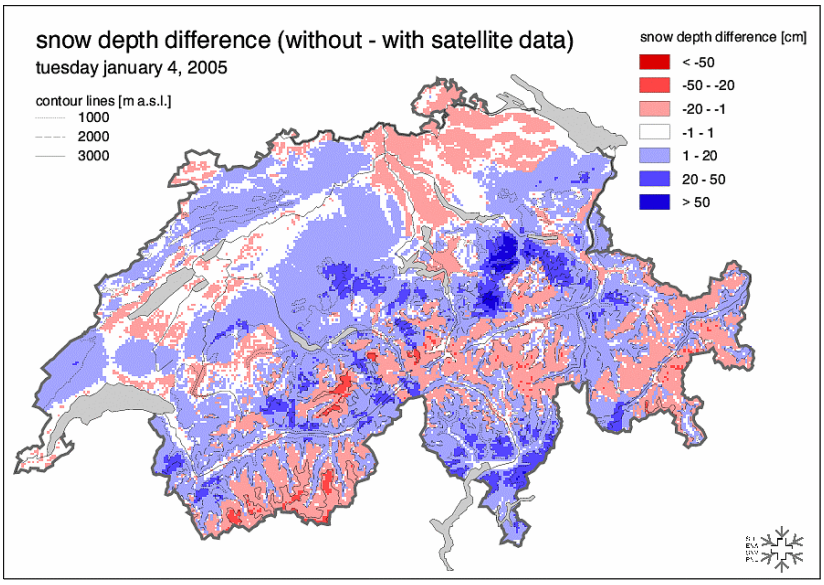

Figure 7: Snow depth difference map from Figures 5 and 6. Dark colours show areas with a high influence of the snow depth calculation including the no snow values from the virtual snow stations.

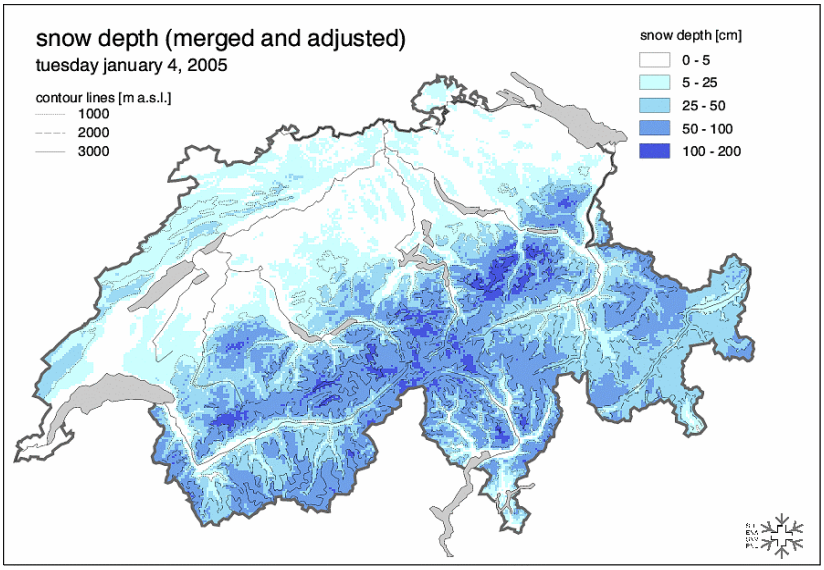

Figure 8: Snow depth map calculated with in situ *snow depth data and no snow values from satellite data, whereof some misclassified virtual stations were excluded from the calculation.*

The virtual snow stations included in the interpolation with a snow depth of zero centimetres are marked as yellow points in Figure 3. Some of these stations fall into pixels that are classified as no snow but surrounded by a greater snow-covered area. These scattered small areas have the effect of a high weight in the calculation of the base and compensation value and result in high differences. These isolated virtual snow stations were identified with the help of adjacent snow depth measurements and erased in a second calculation. The result in Figure 8 and the difference calculated from Figure 5 minus Figure 8 data shown in Figure 9 highlight very good improvements in the

regions identified above when compared visually with the false colour composite (Figure 4) and the binary snow cover map (Figure 3).

The red areas indicating an increase of snow depth are less prominent. The blue areas indicating a decrease of snow depth are closely related to the location of the virtual stations. Excluding the outlier stations from the interpolation leads to smaller differences in the snow depth estimation. In general, the lower altitudes show a decrease and higher altitudes an increase of snow depth compared to the interpolation using snow measurements only.

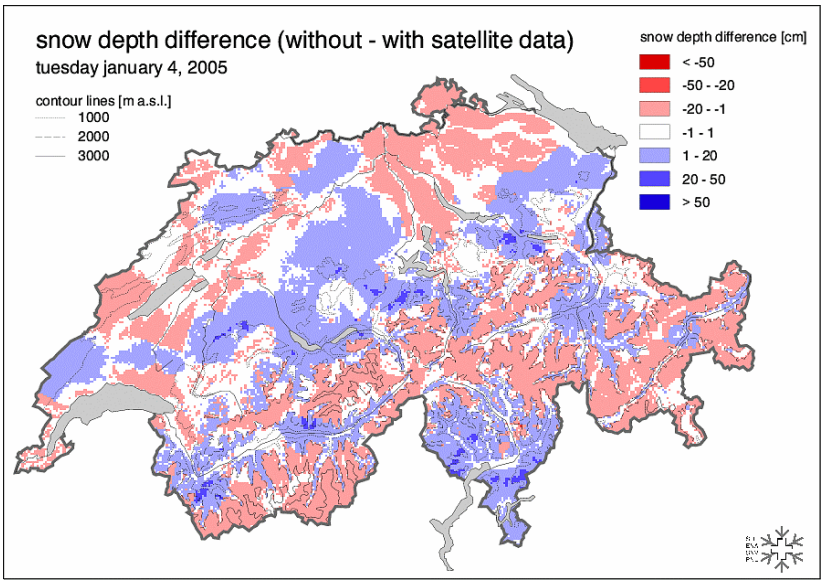

Figure 9: Snow depth difference map from Figure 5 minus Figure 8 data. Excluding isolated virtual snow stations surrounded by larger snow-covered areas from the interpolation leads to lower differences in the snow depth estimation.

CONCLUSIONS AND OUTLOOK

The former interpolation method for area-wide snow depth mapping based on (1) has been substituted by a new approach taking the complex topography of the Alps into account. This was possible because the observation network has been enlarged during the past years. Nevertheless, due to its distribution and reduced operation in certain periods, some areas remain with few snow observations. Therefore, operational snow cover maps from polar-orbiting NOAA satellites are used to fill these gaps. The merging of discrete point field observations with the smaller scale of satellite data is difficult because of the scale differences. The use of a virtual snow station network derived from the binary classified AVHRR data set improves the snow depth interpolation compared to the snow depth map calculated from *in situ* snow depth data only. For the presented case study an increase of snow depth in higher elevation zones was observed, whereas a decrease of snow occurred at lower altitudes. These results are promising and the described approach is already in operational use. The merging of the two data sets is sensitive to isolated virtual snow stations located in a snow-free classified pixel surrounded by larger snow-covered areas. The binary snow cover classification provides useful additional snow information for spatial interpolation of snow depth when cloud contamination is small. The analysis shows that a solid method for snow-no snow classification in the processing of the satellite data is essential to the quality of the final snow depth map. Therefore, an accuracy assessment of the snow cover fraction maps obtains highest priority. The performance of the AVHRR sub-pixel algorithm will be determined using different snow-covered regions in the European Alps. High-spatial resolution data will be used as *ground truth* to calculate the percentage of snow cover for AVHRR 1 km grid cells for an overall error estimation. In this respect special attention will be paid to the effects of the large viewing angle of the AVHRR in the alpine terrain. Further analysis will be carried out to improve the spatial interpolation method used to calculate the area-wide snow depth maps.

ACKNOWLEDGEMENTS

We would like to thank MeteoSwiss for the meteorological data from the Alpine Model (aLMo) as well as the National Centre for Environmental Prediction (NCEP) for supplying meteorological data. We also gratefully appreciate the programming support of Martin Stoffel at the Swiss Federal Institute for Snow and Avalanche Research, Davos (SLF).

REFERENCES

1 Witmer U, P Filliger, S Kunz & P Küng, 1986. Erfassung, Bearbeitung und Kartierung von Schneedaten in der Schweiz (Capture, processing and cartography of snow data in Switzerland) (Geographica Bernensia G25, University of Bern) 215 pp. (in German)

2 Witmer U, 1987. Climatological Atlas of Switzerland, Table (Swiss Meteorological Institute) (in German)

3 Kirchhofer W, 2000. Climatological Atlas of Switzerland, Table 10.7 (Swiss Meteorological Institute) (in German)

4 Auer M, 2003. Regionalisierung von Schneeparametern. Eine Methode zur Darstellung von Schneeparametern im Relief (Master Thesis, University of Bern) 97 pp. (in German)

5 Goodrum G, K B Kidwell & Winston, 2000. NOAA KLM User's Guide. National Environmental Satellite, Data, and Information Services (NESDIS) http://www2.ncdc.noaa.gov/docs/klm/

6 Rahman H & G Dedieu, 1994. SMAC: a simplified method for the atmospheric correction of satellite measurements in the solar spectrum. International Journal of Remote Sensing, 5(1): 105-122

7 Key J, 2002. The Cloud and Surface Parameter Retrieval (CASPR) system for polar AVHRR user's guide. Cooperative Institute for Meteorological Satellite Studies (Madison, WI, University of Wisconsin)

8 Nolin A W, J Dozier & L A K Mertes, 1993. Mapping alpine snow using a spectral mixture modeling technique. Annals of Glaciology, 17: 121-124

9 Simpson J J, J R Stitt & M Sienko, 1998. Improved estimates of the areal extent of snow cover from AVHRR data. Journal of Hydrology, 204(1-4): 1-23

10 Metsämäki S, J Vepsäläinen, J Pullinainen & Y Sucksdorff, 2002. Improved linear interpolation method for the estimation of snow-covered area from optical data. Remote Sensing of Environment, 82(1): 64-78

11 Vikhamar D & R Solberg, 2002. Subpixel mapping of snow cover in forests by optical remote sensing. Remote Sensing of Environment, 84(1): 69-82

12 Romanov P, D Tarley, G Gutman & T Carroll, 2003. Mapping and monitoring snow cover fraction over North America. Journal of Geophysical Research, 108(D16): 8619

13 Salomonson V V & I Appel, 2004. Estimating fractional snow cover from MODIS using the normalized difference snow index. Remote Sensing of Environment, 89: 351-360

14 Rosenthal W & J Dozier, 1996. Automated mapping of montane snow cover at subpixel resolution from the Landsat Thematic Mapper. Water Resources Research, 32(1): 115-130

15 Adams J B , M O Smith & A R Gillespie, 1989. Simple models for complex natural surfaces: a strategy for the hyperspectral era of remote sensing. In International Geoscience and Remote Sensing Symposium (IGARSS). Quantitativ remote sensing: an economic tool for the nineties. (12th Canadian Symposium on Remote Sensing, Vancouver, British Columbia). Proceedings. Vol.1 (New York, Institute of Electrical and Electronics Engineers) 16-21

16 Settle J & N Drake, 1993. Linear mixing and the estimation of ground cover proportions. International Journal of Remote Sensing, 14(6): 1159-1177

17 Roberts D A, M Gardner, R Church, S Ustin, G Scheer & R O Green, 1998. Mapping Chaparral in the Santa Monica Mountains using Multiple Endmember Spectral Mixture Models. Remote Sensing of Environment, 65(3): 267-279

18 Foppa N, S Wunderle, A Hauser, D Oesch & F Kuchen, 2004. Operational sub-pixel snow mapping over the Alps with NOAA-AVHRR data. Annals of Glaciology, 38: 245-252